JOURNAL OF Materials CHEMISTRY

Surface and photochemical properties of Langmuir monolayer and Langmuir–Blodgett films of a spiropyran derivative

Hiroaki Tachibana,*[a] Yasushi Yamanaka[b] and Mutsuyoshi Matsumoto[b]

[a]*Correlated Electron Research Center (CERC), National Institute of Advanced Industrial Science and Technology, 1-1-1 Higashi, Tsukuba 305-8562, Japan. E-mail: h-tachibana@aist.go.jp; Fax: +81-298-61-2586; Tel: +81-298-61-2500*
[b]*Nanotechnology Research Institute, National Institute of Advanced Industrial Science and Technology, Tsukuba 305-8565, Japan*

Received 24th September 2001, Accepted 4th January 2002
First published as an Advance Article on the web 21st February 2002

Langmuir monolayers of an amphiphilic spiropyran, 1′,3′-dihydro-3′,3′-dimethyl-6-nitro-1′-octadecyl-8-docosanoyloxymethylspiro[1-benzopyran-2,2′-indole] (SP1822) on pure water at 30 °C was investigated by measurements of surface pressure–area (π–A) isotherms and Brewster angle microscopy (BAM). The π–A isotherm shows a phase transition at 7.5 mN m^{-1}. The BAM image reveals drastic morphological changes accompanying the phase transition. Many circular domains appear on uniform monolayers. Atomic force microscopy (AFM) images of as-deposited Langmuir–Blodgett (LB) films suggest that the circular domains consist of bilayers. In addition, monolayers are transformed into bilayers during deposition, which result in the formation of further larger circular domains. Furthermore, the relationship between photochemical property and morphology in the SP1822 LB films was characterized by UV-visible spectroscopy and AFM. We have demonstrated that whether J-aggregates are formed upon irradiation with UV light at room temperature is strongly dependent on the morphology of the SP1822 LB films before irradiation.

Introduction

The preparation and photochemical reaction of spiropyran derivatives have been a focus of research aimed at creating switching devices.[1,2] Spiropyran (SP) isomerizes to open colored photomerocyanine (PMC) with a broad absorption band in the visible region upon irradiation with UV light. A number of PMCs with different absorption bands have been developed by changing the skeleton of SP and by introducing various substituents into SP. The photochemical behavior has been investigated in various matrices[3] such as the crystalline state,[4,5] Langmuir–Blodgett (LB) films,[6–9] self-assembled monolayers,[10] vacuum-deposited films,[11] casting films,[12] liquid crystals,[13,14] solution,[15,16] and bilayer membranes dispersed in water.[17]

In particular, the LB technique is interesting, because monolayers with a thickness less than several nanometers can be fabricated onto solid substrates at a molecular level. Much work has been reported on the photochemical reaction at the air–water interface and in deposited LB films of amphiphilic spiropyran derivatives such as 1′,3′-dihydro-3′,3′-dimethyl-6-nitro-1′-octadecyl-8-docosanoyloxymethylspiro[1-benzopyran-2,2′-indole] (SP1822). J-aggregates are induced on irradiation with UV light under external stimuli such as lateral compression at the air–water interface[18–20] and heating of samples on solid substrates,[21,22] which makes spiropyran a potential candidate for photonic applications such as multiple optical memories because of the thermal stability and the sharp absorption band.[23,24] However, most of the photochemical reactions have been studied in mixed LB films with matrices such as fatty acid and *n*-alkane.

Recently, we have succeeded in transferring single-component SP1822 films without matrices by utilizing a high subphase temperature (30 °C). We have been systematically investigating the photochemical properties of spiropyran in single-component SP1822 LB films.[25–27] Many large circular domains are observed in AFM images of the SP1822 LB films, irrespective of the concentration of the SP1822 solution. However, J-aggregate formation upon irradiation with UV light depends strongly on the surface structure of the circular domain before irradiation, which leads to a difference in the temperature for the J-aggregate formation. In the case of a dilute solution, irregularly shaped structures in the center of the circular domains trigger J-aggregate formation upon irradiation with UV light at room temperature. On the other hand, when using a concentrated solution, no such structures are observed on the surface of the circular domains. Instead, heating of the sample during UV irradiation is required for J-aggregate formation.

In this paper, surface pressure–area (π–A) isotherms and Brewster angle microscopy (BAM) of SP1822 were measured to increase the understanding of the formation of the circular domains occurring at the air–water interface. Furthermore, we fabricated single-component SP1822 LB films at various surface pressures. The relationship between the photochemical reaction and morphological changes was investigated by UV-visible spectrocopy and atomic force microscopy (AFM) of the deposited SP1822 LB films.

Experimental

Materials

SP1822 (Nippon Kankoh-Shikiso Kenkyusho Co., Ltd.) was used without further purification. Chloroform of spectroscopic grade (Dojindo Lab.) was used as a spreading solvent.

Monolayer formation

Surface pressure–area (π–A) isotherms were measured with a Lauda Film Balance. The subphase water was purified by distillation after passing through a Milli-Q filtering system. Chloroform solutions of SP1822 at a concentration of 1×10^{-3} M were spread under yellow light conditions onto the pure water at 30 °C. After allowing the solvent to evaporate for

 DOI: 10.1039/b108646b

10 min, the monolayers were compressed at a speed of 5×10^{-2} nm^2 molecule^{-1} min^{-1}.

Brewster angle microscopy (BAM)

Measurement of the macroscopic structure of monolayers on the water surface by Brewster angle microscope (BAM) was carried out in a home-constructed system equipped with a rectangular Teflon trough and a Wilhelmy plate pressure sensor.[28] The BAM system is composed of a 20 mW He–Ne laser, a Gran-Thompson polarizer, an analyzer, a zooming microscope for long distanceworking , and a high sensitivity CCD camera connected to a TV monitor and a video recording system. The π–A isotherms were also measured using the Wilhelmy trough. The results obtained were identical, irrespective of the manner in which the surface pressure was measured.

Atomic force microscopy (AFM)

SP1822 LB films were transferred at a constant surface pressure onto freshly cleaved mica by a vertical dipping method. Atomic force microscopic (AFM) measurements were taken in air using a Seiko SPA300 microscope operating in the noncontact mode using a scanner with 100×100 μm^2 scan range. A silicon tip with a resonant frequency of 28 kHz and a spring constant of 1.9 Nm^{-1} was employed for the observation of surface morphology of single-component SP1822 LB films.

Irradiation

A 500 W high-pressure mercury lamp was used as the source of UV light. The sample was set on a rotating table and 334 nm monochromatic light was used for irradiation at room temperature (25 °C). The UV-visible absorption spectral changes were monitored using a Cary 500 Scan UV-Vis-NIR spectrophotometer.

Results and discussion

Surface pressure–area isotherms

Fig. 1 shows the surface pressure–area (π–A) isotherms of SP1822 on pure water. The change in the slope followed by a plateau region of constant surface pressure is observed at 7.5 mN m^{-1}, corresponding to a first-order phase transition. Upon further compression, the slope increases gradually at the end of the plateau. Finally, the isotherm becomes steep, suggesting a more densely packed structure.

The shape of the isotherm around 7.5 mN m^{-1} depended strongly on the compression speed. A bump in surface pressure at the beginning of the plateau appears above a certain compression speed. The size of the bump is a function of the compression speed, which can be reduced by using a slower compression speed. The bump disappears at a compression speed of 5×10^{-2} nm^2 molecule^{-1} min^{-1} in the present study. The bump in surface pressure is due to a kinetic effect accompanying a slow rearrangement of SP1822 molecules. Brewster angle microscopy (BAM) images support this suggestion as described below.

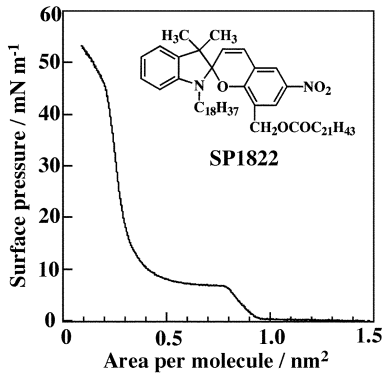

Fig. 1 Surface pressure–area (π–A) isotherms of SP1822 on pure water at 30 °C. The inset shows the chemical structure of SP1822 used in this study.

Brewster angle microscopy

We investigated the morphological changes accompanying the phase transition by measurement of Brewster angle microscopy (BAM). The time dependence of the BAM images after stopping the compression around 7.5 mN m^{-1} is shown in Fig. 2. When the compression is stopped at the beginning of the plateau, one nucleus appears on uniform films immediately accompanying the change in the brightness. Once the nucleation occurs, other nuclei are induced successively in the surrounding regions. Respective nuclei continue to grow up spontaneously with the increase in the holding time, forming circular domains. Finally, the size and the number of the circular domains achieve the saturated state. Many circular domains with uniform size become dominant at the air–water interface after a few tens of minutes. The shape of circular domains remains unchanged even when increasing further the holding time. These results suggest a quite dramatic phase transition of the SP1822 molecules at the air–water interface. Similar morphological changes are also observed during lateral compression up to 10 mN m^{-1}. To follow the detailed morphological changes above 10 mN m^{-1} by BAM is, however, difficult because of the strong brightness in the circular domains.

Atomic force microscopy

We fabricated the SP1822 LB films at various surface pressures above the phase transition. The morphology was investigated by measurement of AFM. Fig. 3 shows AFM images of SP1822 LB films transferred onto mica at 10 mN m^{-1}. The AFM images show many large circular domains with a width of 10–20 μm and a height of 4–5 nm, which are significantly separated from each other and of uniform size. The shape of the domain was identical, irrespective of compression speed, although the size varies slightly. From the cross-section analysis of the height image, the surface of the circular domains is smooth. Only a few small domains of cone-shaped structures are observed between the circular domains. Considering that the molecular length estimated from the CPK model is 2.5 nm, the circular domains probably consist of bilayers.

To confirm whether the films exist between the circular domains, the SP1822 LB films were removed by using a contact AFM. When scratching the regions of the circular domains by the AFM cantilever tip with an applied force of 10^{-9} N, the scratched regions were the same height as those between circular domains. This result indicates that almost all the regions between the circular domains correspond to mica

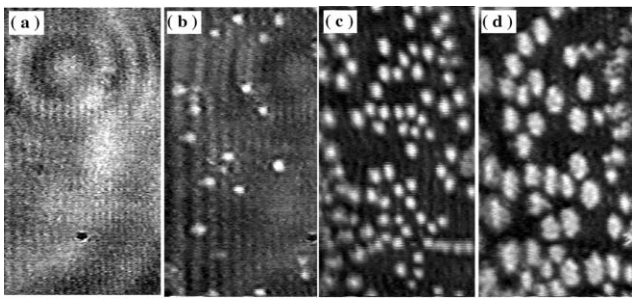

Fig. 2 Time dependence of the Brewster angle microscopy (BAM) image of SP1822 on pure water at 30 °C after stopping the compression around 7.5 mN m^{-1}: (a) 0 min; (b) 1 min; (c) 5 min; (d) 10 min.

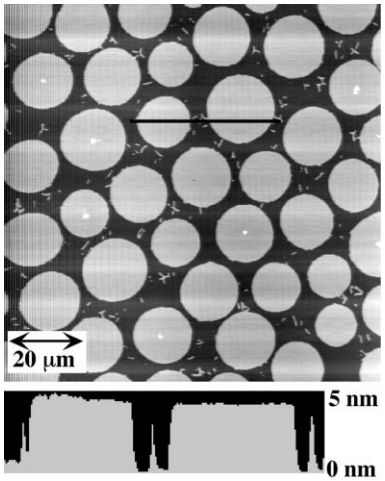

Fig. 3 AFM image (100 μm × 100 μm) of SP1822 LB film transferred at 10 mN m^{-1}. A cross section profile along the black line is shown at the bottom.

substrate. However, when following the change in the BAM images during the continuous compression, the circular domains due to bilayers and the surrounding homogenous monolayers coexist above the phase transition at 7.5 mN m^{-1}. Therefore, it is likely that the rearrangement of the monolayers between circular domains occurs during deposition when transferring SP1822 films at surface pressure above the phase transition onto solid substrates. We propose the deposition process as follows. Almost all the monolayers are incorporated into circular domains accompanying the transformation into the bilayer. The other monolayers crystallize each other and form small domains of cone-shaped structures between the circular domains. Therefore, monolayers do not exist between the circular domains in SP1822 films onto solid substrates.

Fig. 4 shows AFM images of SP1822 LB films at higher surface pressure. The AFM image at 15 mN m^{-1} reveals that the circular domains are densely packed and coalesce partially. The irregularly shaped structures, which correspond to the brighter parts in the AFM image, are observed in the boundary regions of the circular domains at 20 mN m^{-1}. The height was higher than for the circular domains. The structures increase in number and size with the increase in surface pressure. The monolayers between the circular domains may collapse during the continuous compression at the air–water interface and/or the deposition onto solid substrates. Upon compression to 35 mN m^{-1} the circular domains are pushed together in the direction of the compression. Consequently, the irregularly shaped structures are assembled into wire with a length of several hundred micrometers.

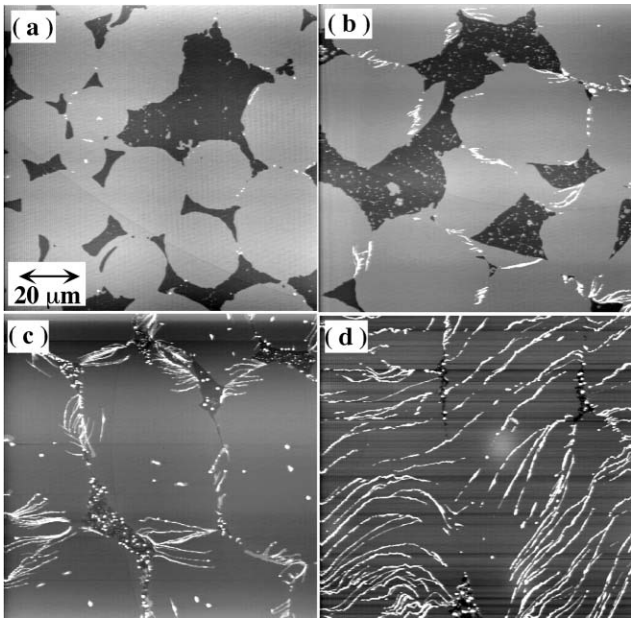

Fig. 4 AFM image (100 μm × 100 μm) of SP1822 LB film: (a) 15 mN m^{-1}; (b) 20 mN m^{-1}; (c) 25 mN m^{-1}; (d) 35 mN m^{-1}.

Photochemical reaction

We investigated photochemical reactions of spiropyran in SP1822 LB films deposited at various surface pressures. UV-visible absorption spectra after reaching the photostationary state upon irradiation with UV light at room temperature are shown in Fig. 5. A broad absorption band appears around 580 nm in the LB films at 10 mN m^{-1}, indicating photoisomerization of SP1822 to monomeric PMC. On prolonged irradiation, only the intensity of the absorption due to monomeric PMC increased without changing the spectral profile. In contrast, the photochemical reaction of SP1822 in LB films at higher surface pressure exhibited different behavior. In addition to the broad absorption due to PMC, a sharp absorption band is observed at 620 nm in the larger wavelength region, corresponding to the J-aggregate of PMC. Furthermore, the intensity of the J-band is enhanced with the increase in the surface pressure. These results indicate that the photochemical reaction depends strongly on the surface pressure.

To clarify the difference in the photochemical reaction, the morphology after irradiation was measured by AFM. Upon irradiation with UV light, the morphological changes were not observed in the LB films at low surface pressure. The morphology remains the initial circular domains even after reaching the photostationary state, although the photoisomerization of SP1822 to PMC occurs into the domains as reported previously.[27] On the other hand, the morphology in the LB films at high surface pressure changes drastically after irradiation, which is due to the J-aggregate formation. The AFM images in the LB films at 25 and 35 mN m^{-1} after reaching the photostationary state upon irradiation with UV light are shown in Fig. 6. Both AFM images show that many tree-like structures are formed in LB films.

Compared to AFM images before irradiation for both LB films at 25 and 35 mN m^{-1} (see Figs. 4c and 4d), it is clear that the tree-like structures spread from the irregularly shaped structures in the boundary regions. Similar morphological changes have been observed in SP1822 LB films fabricated from the dilute solution (0.1 mM).[25,26] These results indicate that the irregularly shaped structures play an important role in the J-aggregate formation upon irradiation with UV light at room temperature, irrespective of preparation conditions.

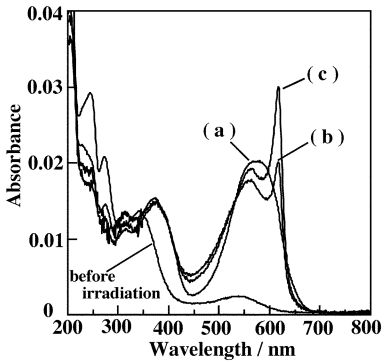

Fig. 5 Change in absorption spectra of SP1822 LB films after reaching the saturated state upon irradiation with UV light: (a) 10 mN m^{-1}; (b) 25 mN m^{-1}; (c) 35 mN m^{-1}.

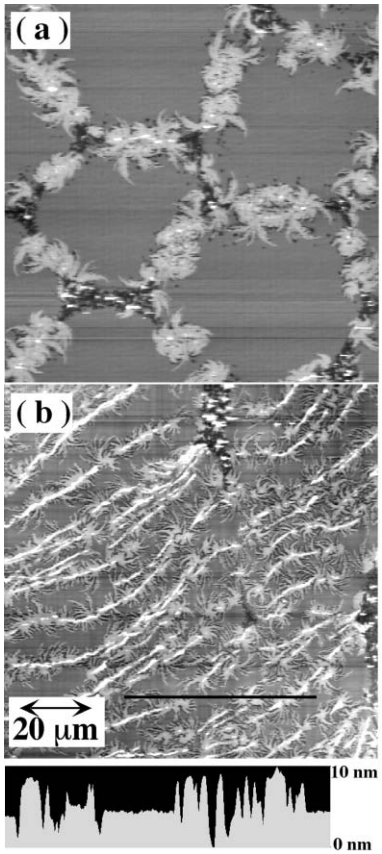

Fig. 6 AFM image (100 μm × 100 μm) of SP1822 LB film after reaching the saturated state upon irradiation with UV light: (a) 25 mN m^{-1}; (b) 35 mN m^{-1}. A cross section profile along the black line in Fig. 6b is also shown.

When zooming around the tree-like structures, many branches with a length of several tens of micrometers were observed in the AFM images. From the cross-section analysis of the height image, the structures accompany the lower regions side by side. The height difference between the highest regions and the lower one is 8–10 nm, which corresponds to twice the height of the domains before irradiation. It is known that the size of J-aggregates in which excitation can migrate without being trapped by defects is less than several tens of nanometers.[29,30] These results indicate that the tree-like structures are formed by the migration and diffusion of many J-aggregates.

Returning to Fig. 5, we can now understand the influence of these morphological features on the photochemical reaction of spiropyran in the SP1822 LB films. When the irregularly shaped structures exist in the LB films before irradiation, PMC molecules are organized into J-aggregates spontaneously upon irradiation with UV light at room temperature. The J-aggregated PMC molecules are further assembled into tree-like structures, irrespective of surface pressure. However, the organization is greater in the LB films at higher surface pressure, which results in the difference in the absorption due to the J-band. Furthermore, the domains are not covered completely by the tree-like structures, indicating that not all the PMCs transform into the J-aggregate. In contrast, the J-aggregate has been observed by heating the SP1822 LB films, which were transferred at 10 mN m^{-1}, up to 50 °C during irradiation.[27] Such further external stimulus is required for transforming monomeric PMC into the J-aggregate when the LB films have no irregular structures. The conditions for J-aggregate formation are associated strongly with the morphology before irradiation.

Conclusions

A Langmuir monolayer of SP1822 at the air–water interface was investigated by measurements of π–A isotherms and BAM. We have revealed that circular domains are formed accompanying phase transition at 7.5 mN m^{-1} in π–A isotherms of SP1822 at 30 °C. AFM images of deposited SP1822 LB films suggest that the circular domains consist of bilayers and the rearrangement from monolayers into bilayers occurs during the deposition. Furthermore, SP1822 LB films were fabricated at various surface pressures. The photochemical reaction of SP1822 upon irradiation with UV light at room temperature depended strongly on the surface pressure. We have investigated the morphological changes after irradiation by AFM, which allowed us to explain the J-aggregate formation upon irradiation with UV light at room temperature. We have demonstrated that the conditions required for J-aggregate formation are determined by the morphology before irradiation.

Acknowledgements

The authors thank Ken-ichi Iimura and Teiji Kato, Utsunomiya University for extensive help with measurement of BAM.

References

1 R. C. Bertelson, in *Photochromism*, ed. G. H. Brown, Wiley, New York, 1971, ch. 3.
2 R. Guglielmetti, in *Photochromism Molecules and Systems*, ed. H. Durr and H. Bouas-Laurent, Elsevier, Amsterdam, 1990, ch. 8.
3 V. A. Krongauz, in. *Photochromism Molecules and Systems*, ed. H. Durr, and H. Bouas-Laurent, Elsevier, Amsterdam, 1990, ch. 21.
4 S. Benard and P. Yu, *Chem. Commun.*, 2000, 65.
5 S. Benard and P. Yu, *Adv. Mater.*, 2000, **12**, 48.
6 E. E. Polymeropoulos and D. Mobius, *Ber. Bunsenges. Phys. Chem.*, 1979, **83**, 1215.
7 M. Morin, R. M. Leblanc and I. Gruda, *Can. J. Chem.*, 1980, **58**, 2038.
8 R. Vilanove, H. Hervet, H. Gruler and F. Rondelez, *Macromolecules*, 1983, **16**, 825.
9 D. A. Holden, H. Ringsdrof, V. Deblauwe and G. Smets, *J. Phys. Chem.*, 1984, **88**, 716.
10 J. M. Galvin and G. B. Schuster, *Supramolecular Sci.*, 1998, **5**, 89.
11 S. Hayashida, H. Sato and S. Sugawara, *Jpn. J. Appl. Phys.*, 1985, **24**, 1436.
12 H. Tomioka, F. Inagaki and T. Itoh, *J. Photopolym. Sci. Technol.*, 1990, **3**, 83.
13 I. Cebrara, V. Krongauz and H. Ringsdorf, *Angew. Chem., Int. Ed. Engl.*, 1988, **26**, 1178.
14 A. Y. Bobrovsky, N. I. Boiko and V. P. Shibaev, *Adv. Mater.*, 1999, **11**, 1025.
15 K. Kimura, T. Yamashita, M. Kaneshige and M. Yokoyama, *J. Chem. Soc., Chem. Commun.*, 1992, 969.
16 M. Tanaka, K. Kamada, H. Ando, T. Kitagaki, Y. Shibutani and K. Kimura, *J. Org. Chem.*, 2000, **65**, 4342.
17 T. Seki, K. Ichimura and E. Ando, *Langmuir*, 1988, **4**, 1068.
18 E. Ando, M. Suzuki, K. Moriyama and K. Morimoto, *Thin Solid Films*, 1989, **178**, 103.
19 E. Ando, K. Moriyama, K. Arita and K. Morimoto, *Langmuir*, 1990, **6**, 1451.
20 A. Miyata, Y. Unuma and Y. Higashigaki, *Bull. Chem. Soc. Jpn.*, 1991, **64**, 1719.
21 E. Ando, J. Miyazaki, K. Morimoto, H. Nakahara and K. Fukuda, *Thin Solid Films*, 1985, **133**, 21.
22 A. Miyata, Y. Unuma and Y. Higashigaki, *Bull. Chem. Soc. Jpn.*, 1993, **66**, 993.
23 E. Ando, J. Miyazaki, K. Moritomo, H. Nakahara and K. Fukuda, in *Proc. Int. Symp. on Future Electron Devices*, Research and Development Association for Future Electron Devices, Tokyo, 1985, p. 47.
24 Z.-Z. Gu, S. Hayami, Q.-B. Meng, T. Iyoda, A. Fujishima and O. Sato, *J. Am. Chem. Soc.*, 2000, **122**, 10730.
25 H. Tachibana, Y. Yamanaka, H. Sakai, M. Abe and M. Matsumoto, *Chem. Lett.*, **2000**, 1182.

26 H. Tachibana, Y. Yamanaka, H. Sakai, M. Abe and M. Matsumoto, *Mol. Cryst. Liq. Cryst.*, 2000, **345**, 149.
27 H. Tachibana, Y. Yamanaka and M. Matsumoto, *J. Phys. Chem. B*, 2001, **105**, 10282.
28 T. Kato, A. Tatehana, N. Suzuki, K. Iimura and K. Iriyama, *Jpn. J. Appl. Phys.*, 1995, **34**, L911.
29 D. A. Higgins, J. Kerimo, D. A. VandenBout and P. F. Barbara, *J. Am. Chem. Soc.*, 1996, **118**, 4049.
30 T. Tani, L. Yi, M. Vacha, F. Sasaki and S. Kobayashi, *Mol. Cryst. Liq. Cryst.*, 1996, **291**, 251.